Precambrian Research 173 (2009) 70–78

Contents lists available at ScienceDirect

Precambrian Research

journal homepage: www.elsevier.com/locate/precamres

NanoSIMS: Insights to biogenicity and syngeneity of Archaean carbonaceous structures

Dorothy Z. Oehler[a,*], François Robert[b], Malcolm R. Walter[c], Kenichiro Sugitani[d], Abigail Allwood[e], Anders Meibom[b], Smail Mostefaoui[b], Madeleine Selo[b], Aurélien Thomen[b], Everett K. Gibson[a]

[a] Astromaterials Research and Exploration Science Directorate, NASA–Johnson Space Center, 2101 NASA Parkway, Houston, TX 77058, USA
[b] Laboratoire d'Etude de la Matière Extraterrestre, Muséum National d'Histoire Naturelle, USM 0205 (LEME), Case Postale 52, 61, Rue Buffon, Paris 75005, France
[c] Australian Centre for Astrobiology, University of New South Wales, Kensington, NSW 2052, Australia
[d] Department of Environmental Engineering and Architecture, Graduate School of Environmental Studies, Nagoya University, Nagoya 464-8601, Japan
[e] Planetary Science, Jet Propulsion Laboratory, M/S 183-301, 4800 Oak Grove Drive, Pasadena, CA 91109, USA

ARTICLE INFO

Article history:
Received 25 August 2008
Received in revised form 11 January 2009
Accepted 20 January 2009

Keywords:
NanoSIMS
Archaean
Pilbara
Organic microfossil
Bitter Springs
Proterozoic

ABSTRACT

NanoSIMS is a relatively new technology that is being applied to ancient carbonaceous structures to gain insight into their biogenicity and syngeneity. NanoSIMS studies of well preserved organic microfossils from the Neoproterozoic (~0.8 Ga) Bitter Springs Formation have established elemental distributions in undisputedly biogenic structures. Results demonstrate that sub-micron scale maps of metabolically important elements (carbon [C], nitrogen [measured as CN ion], and sulfur [S]) can be correlated with kerogenous structures identified by optical microscopy. Spatial distributions of C, CN, and S in individual microfossils are nearly identical, and variations in concentrations of these elements parallel one another. In elemental maps, C, CN, and S appear as globules, aligned to form remnant walls or sheaths of fossiliferous structures. The aligned character and parallel variation of C and CN are the strongest indicators of biogenicity.

Nitrogen/carbon atomic ratios (N/C) of spheroids, filaments, and remnants of a microbial mat suggest that N/C may reflect original biochemical differences, within samples of the same age and degree of alteration. Silicon (Si) and oxygen (O) maps illustrate that silica is intimately interspersed with organic carbon of the microfossils. This relationship is likely to reflect the process of silica permineralization of biological remains and thus may be an indicator of syngeneity of the fossilized material with the mineral matrix.

The NanoSIMS characterization of Bitter Springs microfossils can be used as a baseline for interpreting less well preserved carbonaceous structures that might occur in older or even extraterrestrial materials. An example of such an application is provided by comparison of Bitter Springs results with NanoSIMS of Archaean carbonaceous structures from Western Australia, including a spheroid in the ~3 Ga Farrel Quartzite and material in a secondary vein in the 3.43 Ga Strelley Pool Chert. Results reinforce a biogenic, syngenetic interpretation for the Archaean spheroid.

NanoSIMS has several advantages in the study of ancient organic materials: the technique allows characterization of extremely small structures that are present in low concentrations; organic matter does not have to be isolated by acid treatment but can be analyzed in polished thin section; preparation is simple; samples are minimally altered during analysis; results provide sub-micron scale spatial distribution coupled with concentration information for at least five elements; the biologically important elements of carbon and nitrogen can be assessed; and the ability to study organic remains *in situ* permits petrographic assessment of spatial relationships between organic matter and mineral constituents. These advantages could be of significant benefit for interpretation of poorly preserved and fragmentary carbonaceous remains that might occur in some of Earth's oldest samples as well as in meteorites or extraterrestrial material brought to Earth in future planetary missions.

1. Introduction

As the study of biological evolution encompasses ever older sediments, interpretations are increasingly dependent on poorly preserved materials. In some samples, fragmentary bits of organic

* Corresponding author. Tel.: +1 281 483 4249; fax: +1 281 483 1573.
E-mail address: dorothy-oehler@comcast.net (D.Z. Oehler).

0301-9268/$ – see front matter © 2009 Elsevier B.V. All rights reserved.
doi:10.1016/j.precamres.2009.01.001

matter may be the only materials available for analysis. While such fragments would lack the familiar three-dimensional morphologies associated with well preserved microfossils, some of those fragments could be of biological derivation. Other organic fragments may be abiotic, formed by hydrothermal or Fischer–Tropsch type reactions or perhaps delivered to Earth by meteorites, during the earliest history of our planet. Consequently, it is possible that mixtures of biogenic and non-biogenic organic remains may co-exist in some of Earth's oldest sediments, and it is of considerable importance that techniques be developed to assess biogenicity in poorly preserved, fragmentary materials.

Studies of Archaean materials exemplify these issues. Samples frequently are poorly preserved; they also are fractured and contain veins of epigenetic hydrothermal material that co-exist with syngenetic organic remains. Their great age also allows for the possibility that biogenic organic materials might be mixed with abiotic organics. This complexity argues for use of analytical methods that can be applied to individual, *in situ* fragments of organic matter, where chemical characterization can be combined with determination of spatial relationships to minerals, veins, fractures, and other organic inclusions.

Comparable problems will arise in the search for evidence of life beyond Earth. Meteorites or planetary sediments brought to Earth in future missions similarly may contain organic materials of diverse origins, including both abiotic and potentially biological derivations. In addition, contamination with terrestrial organic matter is a major concern and identification of syngenetic materials will be critically important. Finally, even if syngenetic biogenic material were abundant in an extraterrestrial sample, the chance that such material would be well preserved is remote. On Earth, paleontologists search the globe for formations which might contain well preserved, ancient microfossils. When such deposits are located, preservation is typically erratic. Samples may be collected from many localities, but reasonably preserved microfossils usually are limited to a few zones. Even in samples from these few zones, well preserved specimens typically constitute only a small percentage of the organic material present. Accordingly, it is unlikely that organic remains that might be found in extraterrestrial samples would be optimally preserved, and assessments of the origin and significance of such organic constituents most probably will be made on poorly preserved and fragmentary specimens.

NanoSIMS is a relatively new technique that has the potential of addressing biogenicity and syngeneity of small fragments of carbonaceous material. Previous work, using SIMS (Secondary Ion Mass Spectrometry) has shown that stable carbon isotopic composition can be determined for individual Proterozoic microfossils and that results have bearing on the affinities of those microstructures (House et al., 2000). In addition, Mojzsis et al. (1996) used SIMS to evaluate the carbon isotopic composition of 5 μm-sized carbonaceous inclusions within apatite grains occurring in ~3.8 Ga, Archaean sediments. NanoSIMS is a Secondary Ion Mass Spectrometer that has been optimized for sub-micron scale spatial resolution. Carbon isotopic composition can be determined at resolutions of 100–500 nm, and chemical element distributions can be determined at resolutions approaching 50 nm. This capability to obtain elemental and isotope data at sub-micron resolution is particularly well suited to analysis of individual microstructures in ancient sediments.

NanoSIMS additionally offers the possibility of studying organic matter *in situ*, within polished thin sections, along with the ability to analyze light elements, such as carbon and nitrogen, which are critical for assessment of biogenicity. Together, the advantages of NanoSIMS (small sample size, *in situ* analysis, sub-micron resolution, minimal sample alteration during analysis, and ability to map biologically important elements) afford the possibility of assessing fragments of poorly preserved organic materials, such as are likely to occur in some of Earth's oldest sediments and in extraterrestrial materials.

The first, in-depth NanoSIMS characterization of ancient organic microfossils was carried out on well preserved microfossils from the Neoproterozoic (~0.8 Ga) Bitter Springs Formation of Australia (Oehler et al., 2006). Results demonstrate elemental distributions of undisputedly biogenic material and serve as a baseline against which less well preserved remains can be compared. To illustrate the applicability of NanoSIMS to assessment of poorly preserved structures, Bitter Springs results are compared here to NanoSIMS characterization of two Archaean carbonaceous structures from the Pilbara of Australia: An organic spheroid from the ~3 Ga Farrel Quartzite and material in a secondary, hydrothermal vein from the 3.43 Ga Strelley Pool Chert (Oehler et al., 2008a–c).

This paper provides the first detailed report of NanoSIMS results for an Archaean microstructure that has been considered as a potential microfossil. Our work has concentrated on elemental composition for carbon, nitrogen, silicon and oxygen (Oehler et al., 2008a–c). Carbon and nitrogen are most valuable for assessing organic composition and biogenicity. Nitrogen is a biologically fixed element and rarely occurs in minerals; it, therefore, can be an indicator of biogenicity when its distribution parallels that of the carbon. Silicon and oxygen distributions appear to reflect silicification of organic materials in chert, and this relationship, as described below, provides insights into the syngeneity of the organic material. Sulfur composition was determined but not reported here, as it may reflect various, biological and non-biological diagenetic processes (Oehler et al., 2006) and its relevance to biogenicity or syngeneity is not clear. Carbon isotopic composition from NanoSIMS is similarly not included, as initial isotopic values measured on the Archaean materials had large error bars and the possibility that the samples might have included minute bits of contamination (Robert et al., 2008), is under continuing investigation.

2. Materials and methods

Analysis was performed on 30 μm thick, polished thin sections. If the cherts were not highly fractured, they were mounted to the glass with a mounting medium but not impregnated with epoxy. If the cherts were fractured, they were additionally embedded in epoxy. Blue dye was added to the epoxy to facilitate recognition of epoxy penetration by optical microscopy in thin section. Preparation without epoxy is possible in many cherts that are not highly fractured. Samples described herein include 1) chert, collected by D.Z. Oehler from the ~0.8 Ga Bitter Springs Formation (Ellery Creek locality) of Australia; 2) chert, collected by K. Sugitani from the ~3 Ga Farrel Quartzite (Mt. Grant locality; Sugitani et al., 2007) of the Pilbara in Western Australia; and 3) chert, collected by A. Allwood, from Member 4 of the 3.43 Ga Strelley Pool Chert (Allwood et al., 2006) of the Pilbara. Member 4 is a silicified clastic/volcaniclastic unit above the stromatolitic facies recently reported from Member 2 (Allwood et al., 2006). Rare-earth-element analyses suggest the onset of hydrothermal activity in Member 4, and material in a vein was used as an example of secondary, hydrothermal carbon.

Individual microstructures were located within the thin sections using optical microscopy. Specimens at the top of the section were selected for NanoSIMS and photographed using an Olympus BX60 Research, Polarizing Optical Microscope, outfitted with a Nikon DXM 1200F Digital Camera; photomicrographs were taken in transmitted and reflected light, and sketch maps were constructed for use with the photographs for locating the specimens in the NanoSIMS. Photomicrographic focal series were taken from the top of the thin section to the base of the structures of interest in transmitted light, using a 100 × oil immersion lens and Cargill type DF immersion oil (Formula Code 1261). The thin section was subse-

quently cleaned by ultrasonication five times with reagent-grade ethanol for 2 minutes, each time. The sample was dried in a 60 °C oven for 1 h to drive off solvents and coated with about 300 Å of gold. It was assumed that the ultrasonication procedure was adequate to remove traces of immersion oil. This assumption is reasonable in view of the facts that (1) initial sputtering by NanoSIMS removes surface contamination before data are collected, and none of the structures imaged resides in a crack in the thin section, where traces of immersion oil conceivably could remain after sputtering, (2) the NanoSIMS carbon maps are mirrored by nitrogen and sulfur maps and thus are suggestive of sedimentary organic matter rather than immersion oil (which is composed only of hydrocarbons and lacks nitrogen and sulfur), and (3) there is a one-to-one correspondence of the carbon, sulfur, and nitrogen maps with optical microscopic images of the kerogenous structures.

Chemical maps were produced with the Cameca NanoSIMS 50 at the Muséum National d'Histoire Naturelle in Paris, France. Using a focused primary beam of cesium (Cs^+), secondary ions of $^{12}C^-$, $^{12}C^{14}N^-$, $^{32}S^-$, $^{28}Si^-$, and $^{16}O^-$ were sputtered from the sample surface and detected simultaneously (multicollection-mode) in electron-multipliers at a mass-resolving power of ~4,500 ($M/\Delta M$). At this mass-resolving power, the measured secondary ions were resolved from potential interference by other ions or molecules that fall close in mass to the ions of interest. Because nitrogen is measured as CN^-, it can only be detected in the presence of carbon. Images were obtained from a presputtered area by stepping the primary beam across the sample surface. Presputtering is done to clean the surface of contaminants before analysis, remove the conductive coating, implant Cs^+ ions in the material to be analyzed, and reach a steady state of ion emission. The primary beam was focused to a spot size of ~50–100 nm, and the step size was adjusted so that it was slightly smaller than the primary beam.

N/C atomic ratios were obtained from measured $^{12}C^{14}N^-$ and $^{12}C^-$ yields by normalization to a kerogen standard that was prepared from the Eocene Green River Shale (for the Bitter Springs sample) or charcoal (for the Archaean sample). The kerogen of the standard was extracted by standard HF–HCl maceration and chemically analyzed for N/C (Beaumont and Robert, 1999). The $^{12}C^{14}N^-/^{12}C^-$ ratio of the standard was then measured in the NanoSIMS using operating conditions identical to those used for analyzing the Precambrian structures. Calibration between the measured $^{12}C^{14}N^-/^{12}C^-$ ratio from NanoSIMS and the chemically determined N/C atomic ratio for the standard was then used to convert measured $^{12}C^{14}N^-/^{12}C^-$ ratios of the Precambrian structures to N/C atomic ratios. NanoSIMS results were processed using L'Image software developed by L. Nittler, Carnegie Institution of Washington, Washington D.C.

3. Results

3.1. NanoSIMS of microfossils in the Neoproterozoic, ~0.8 Ga Bitter Springs Formation

NanoSIMS characterization of microfossils from the Bitter Springs Formation (Oehler et al., 2006) shows that carbon (C) nitrogen (measured as CN), and sulfur (S) distributions can be correlated with structures identified by optical microscopy. Spatial distributions of C, CN (Fig. 1A–D) and S (S not shown) in individual microfossils are nearly identical and variations in concentrations of these elements parallel one another (Fig. 1B, C; also see generally uniform CN/C ratio in Fig. 1D). In elemental maps, C, CN, and S appear as globules that are partially contiguous and aligned to form remnant walls or sheaths of fossiliferous structures (e.g., see C and CN in Fig. 1B, C). The aligned occurrence and parallel variation in C and CN distributions are the strongest indicators of biogenicity.

Nitrogen/carbon atomic ratios (N/C) of the microfossils were determined by measuring CN/C ratios with the NanoSIMS (which are illustrated in Fig. 1) and then correcting the measured CN/C values to atomic N/C ratios by it comparison with a standard (as described in the Materials and Methods Section). This was done with the Bitter Springs microfossils (Oehler et al., 2006) and their resultant N/C atomic ratios are "kerogen-like," in that they are generally within the range of 0.0015-0.03 reported for bulk kerogens from a suite of Precambrian cherts (Beaumont and Robert, 1999). Because all microfossils analyzed were in the same thin section, diagenetic history of each is similar and differences in N/C ratios of filaments, spheroids, and a microbial mat are likely to reflect differences in their respective biochemical precursors (Oehler et al., 2006). The N/C ratios of the Bitter Springs spheroids range from 0.0073 to 0.0133. While this range is much lower than that of modern bacteria (0.15–0.28; Fagerbakke et al., 1996; Fukuda et al., 1998), it is likely that the lower N/C ratios of the spheroids, and Precambrian kerogens reported by Beaumont and Robert (1999), probably reflect a combination of unique Precambrian organisms, diagenetic alteration, and microbial degradation (Oehler et al., 2006).

Silicon (Si) and oxygen (O) distributions appear to mimic C and CN distributions in these microfossils (Fig. 2). Although it might be expected that the Si and O of the chert matrix would be prominent in the Si and O maps, that is not the case. Profiles across three filaments (Fig. 2D, E) show that the Si and O responses associated with these microfossils are 2–3 times higher than in the surrounding chert. Moreover, this type of relationship continues with depth in the thin section. After initial NanoSIMS analyses of spheroidal microfossils (Fig. 2F), intense sputtering into two of the spheroids achieved a lower plane of investigation in the NanoSIMS by more than 1 μm (compare Fig. 2F with G). Elemental maps were acquired again (Fig. 2G, H), and Si and O (O not shown) responses in these intensely sputtered regions continued to be significantly higher in association with the kerogen of the cell wall than in association with the silica of the chert matrix.

3.2. NanoSIMS of a small spheroid in the Archaean, ~3 Ga Farrel Quartzite

NanoSIMS analysis of a small spheroid in the Farrel Quartzite (Fig. 1E–H) was conducted in 2007 (Oehler et al., 2008a–c). C, CN, and S in the small spheroid have a one-to-one correspondence with the structure observed by optical microscopy, and variations in C and CN concentrations parallel one another (Fig. 1F, G; also see generally uniform CN/C ratio in Fig. 1H). The C, CN, and S responses (S not shown) correspond to aligned globular concentrations that are partially contiguous and appear to constitute a wall-like boundary of the structure. N/C ratios for the spheroidal structure range from 0.0125 to 0.05.

Si and O maps demonstrate higher concentrations of these elements in association with carbonaceous material of the spheroid than in association with the surrounding chert (Fig. 3A–C).

3.3. NanoSIMS of carbonaceous material in a vein in the 3.43 Ga Strelley Pool Chert

NanoSIMS C and CN maps of dark, opaque material in a vein are illustrated in Fig. 1I–L. This vein is a secondary, epigenetic structure which cuts through and offsets the primary chert matrix and kerogen in that matrix (Fig. 1I). Although there is a correspondence between C and the material imaged by optical microscopy, CN does not correlate with optically imaged particles. The C of the dark particles of C are angular, separate from one another, and spatially dispersed in the vein without apparent alignment to form any cohesive, wall-like or enveloping structures. The particles are composed of C, CN and S (S not shown), but compared to the Archaean

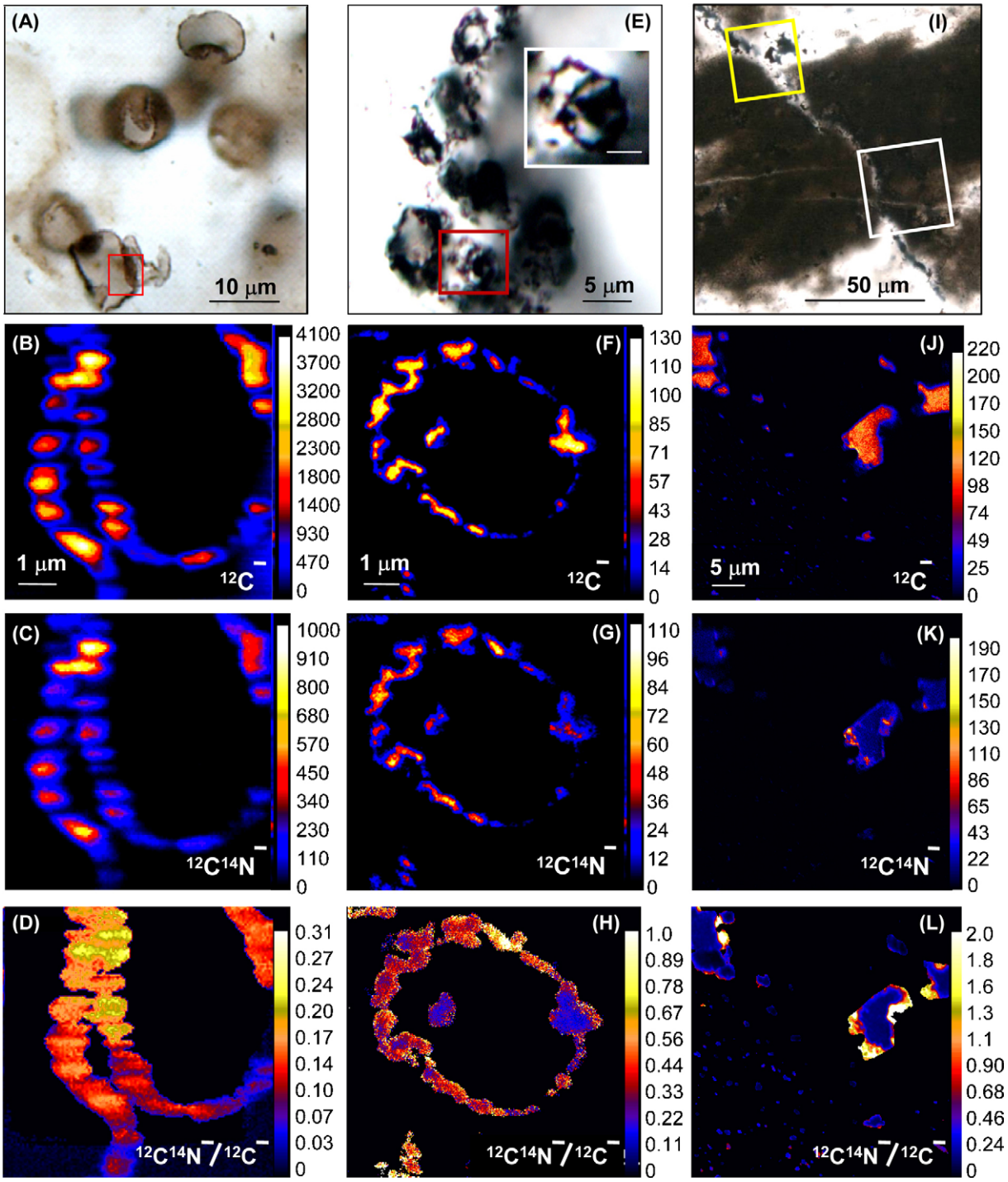

Fig. 1. Comparisons of NanoSIMS responses for structures in polished thin sections of cherts from the ~0.8 Ga Bitter Springs Formation (A–D), the ~3 Ga Farrel Quartzite (E–H), and Member 4 of the 3.43 Ga Strelley Pool Chert (I–L). (A) Optical photomicrograph of a cluster of Bitter Springs spheroidal microfossils; red rectangle shows the area imaged in NanoSIMS element (B, C) and CN/C ratio (D) maps. (E) Optical photomicrograph of a cluster of spheroidal structures in the ~3 Ga Farrel Quartzite; red rectangle shows the structure imaged in NanoSIMS element (F, G) and CN/C ratio (H) maps; white rectangle in (E) is an insert, showing the spheroidal structure imaged in (F–H) at approximately the same focal plane as in (F–H); white scale bar in the insert is 2 μm; (I) Optical photomicrograph of carbonaceous material in a secondary, hydrothermal vein in the 3.43 Ga Strelley Pool Chert; yellow rectangle shows the area imaged in NanoSIMS element (J, K) and CN/C ratio (L) maps; white rectangle is the area imaged in Fig. 4. Color bars and scales on the NanoSIMS maps indicate yield of ions (intensity of response). Scales on images are set by the image processing software. Scale bar in (B) applies to (B–D); scale bar in (F) applies to (F–H); scale bar in (J) applies to (J–L). C, carbon; CN, nitrogen measured as CN ion.

spheroid, they are nitrogen-poor (compare Fig. 1C, G and K). The variations in concentrations of C and CN appear to be antithetic: that is, when concentration of C is high, CN is low, and vice versa (compare Fig. 1J with K; also see CN/C ratio in Fig. 1L). The large carbonaceous particles generally have a C yield of about 100, but at their peripheries, a 0.5–1 μm rim occurs with a much lower yield of about 30 (Fig. 1J); this rim is characterized by relatively high concentrations of CN (Fig. 1K). N/C ratios for the carbonaceous particles (excluding the rims with low C yields) range from 0.003 to 0.019.

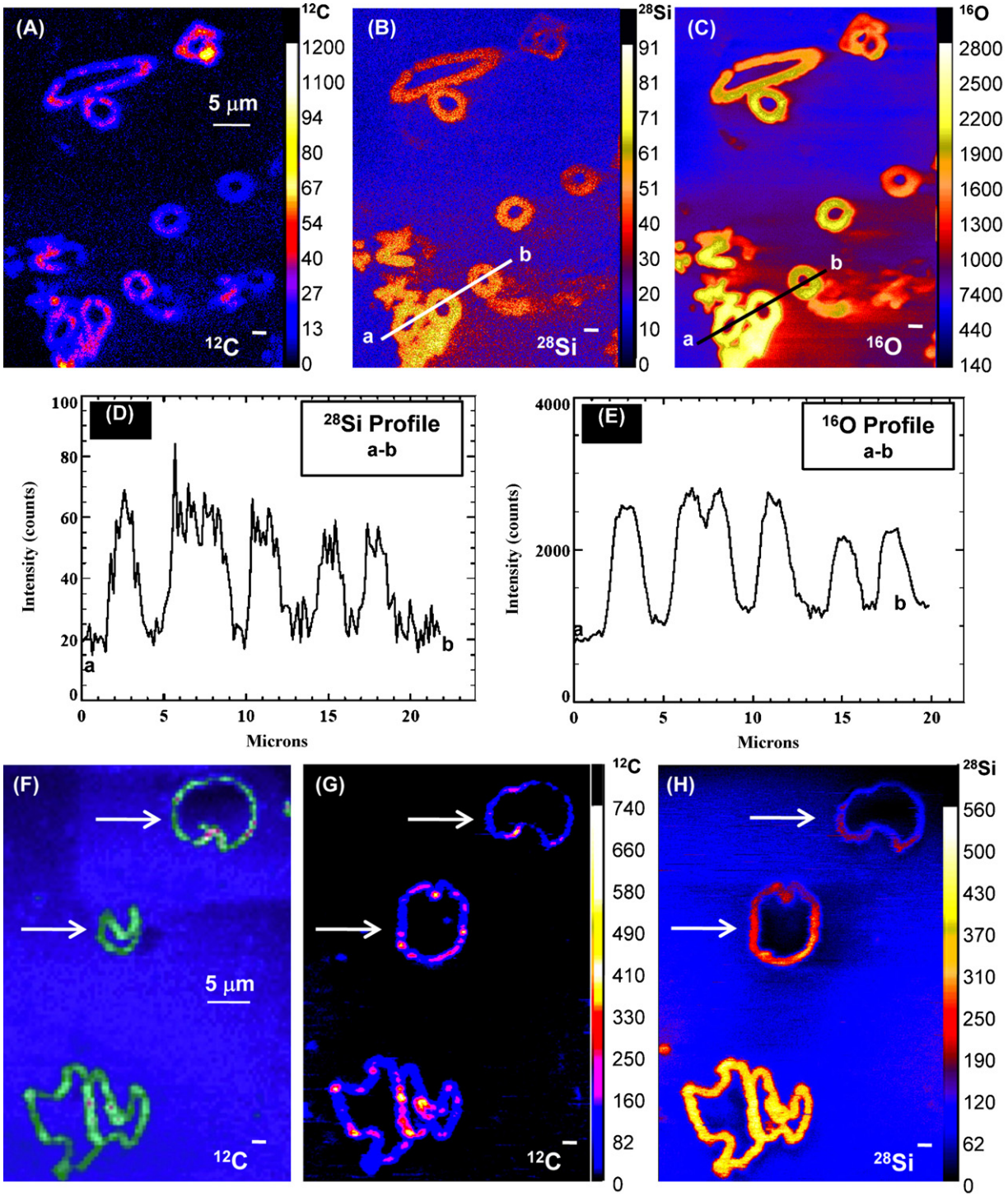

Fig. 2. NanoSIMS data illustrating occurrence of silicon and oxygen in carbonaceous microfossils in chert from the Bitter Springs Formation. (A–C) Filamentous microfossils, showing remnant cyanobacterial sheaths cut in cross section and longitudinal section. Lines a–b in (B) and (C) are the lines of profile for the data shown in (D, E). (D, E) Profiles of intensity of NanoSIMS response for silicon (D) and oxygen (E) along the lines, a–b, shown in (B) and (C). (F–H) Spheroidal microfossils showing remnant microbial cell walls. (F) NanoSIMS image from the top of the thin section. (G, H) NanoSIMS images after intense sputtering on the central area to a lower focal plane in the thin section (arrows point to the cells sputtered). The oxygen response (not shown) is similar to that of silicon. Color bars and scales on the NanoSIMS element maps indicate yield of ions (intensity of NanoSIMS response). Scales on images are set by the image processing software. A color bar was not acquired for (F). Scale bar in (A) applies to (A–C); scale bar in (F) applies to (F–H). C, carbon; Si, silicon; O, oxygen.

The relationships between Si and O and the dark particles are illustrated in Figs. 3D–F and 4. The Si maps, especially, show little enhancement of response above that in the matrix of the chert. The O map in Fig. 3F does show enhancement at the boundaries of the dark particles, but that enhancement occurs mainly in the rims where C yield is lowest and CN yield is highest (compare Fig. 3F with Figs. 3D, 1K and L). Another example of the particles in the vein is shown in Fig. 4; here the O distribution map shows minimal enhancement of response associated with the carbonaceous particles (compare Fig. 4B with Fig. 4D).

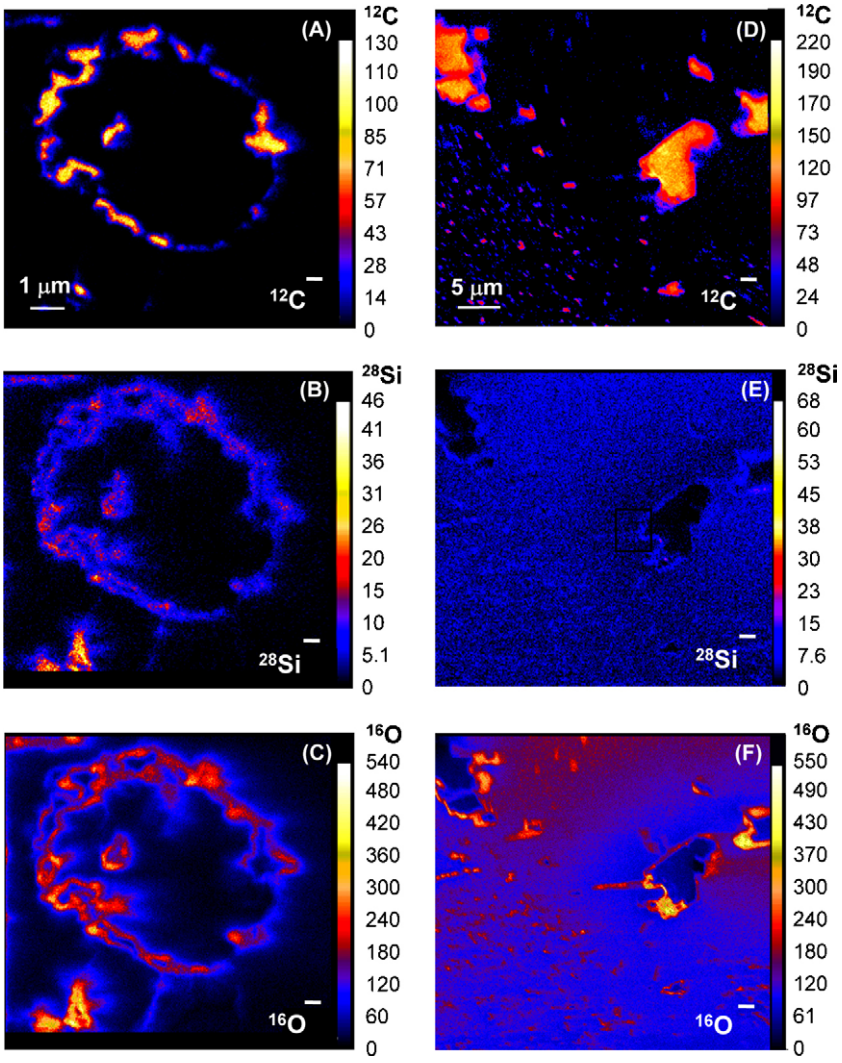

Fig. 3. NanoSIMS images illustrating silicon and oxygen associated with carbonaceous in structures in polished thin sections of Archean cherts. (A–C) Small spheroid in the ~3 Ga Farrel Quartzite; area imaged in (A–C) is shown by rectangles in Fig. 1E. (D–F) Carbonaceous particles in a secondary vein from Member 4 of the 3.43 Ga Strelley Pool Chert; area imaged in (D–F) is shown by yellow rectangle in Fig. 1G. Color bars and scales on the NanoSIMS element maps indicate intensity of NanoSIMS response. Scales on images are set by the image processing software. Scale bar in (A) applies to (A–C); scale bar in (D) applies to (D–F). C, carbon; Si, silicon; O, oxygen.

4. Discussion

The microbiota of the Neoproterozoic Bitter Springs Formation is exceptionally well preserved (Schopf, 1968; Schopf and Blacic, 1971) and there is no doubt that the organic microstructures are of biological origin. Therefore, NanoSIMS results from Bitter Springs microfossils can serve as a baseline for assessing biogenicity of less well preserved materials.

Several examples of less well preserved materials have been described by Sugitani et al. (2007) in Archaean cherts of the ~3 Ga Farrel Quartzite from the Pilbara of Western Australia. While those authors concluded that many of the structures in the Farrel Quartzite are likely to be of biological derivation, their interpretation was cautious, as the structures are relatively poorly preserved and of great age. If biogenicity and syngeneity could be substantiated, this material would represent one of the oldest known microbiotas and would add substantially to knowledge of the early biosphere. As a follow-up, therefore, NanoSIMS element distributions of small spheroids from the Farrel Quartzite were compared with element distributions of both Bitter Springs spheroids and secondary carbon in a hydrothermal vein in the 3.43 Ga Strelley Pool Chert.

NanoSIMS comparisons illustrate several similarities between the Bitter Springs spheroids and the Archaean spheroid (Fig. 1): These include the one-to-one correspondence of the C, CN, and S distributions with the kerogenous structures imaged in optical photomicroscopy; the nearly identical distributions of each of these elements; parallel variations of C and CN, and the globular, partially contiguous, and aligned character of the element concentrations.

One of the most basic characteristics of living systems is the presence of cellular envelopes, such as walls and membranes. Such bounding structures control diffusion of chemicals into and out of cells, and even fragmentary remains of walls would be expected to retain traces of that aligned character. NanoSIMS maps of the Bitter Springs microfossils exemplify such enveloping structures (Fig. 1B, C), and the aligned C and CN globules of the Archaean spheroid from the Farrel Quartzite (Fig. 1F, G) similarly may reflect wall-like structures of ancient cells. In addition, the parallel variations in the concentrations of CN and C in both the Bitter Springs and Archaean spheroids (exemplified by the relatively uniform CN/C ratio images in Fig. 1D and H) are likely to reflect a common origin for C and N which would be consistent with a biological derivation. Together, the aligned nature of the C and CN globules and the parallel variations in C and CN concen-

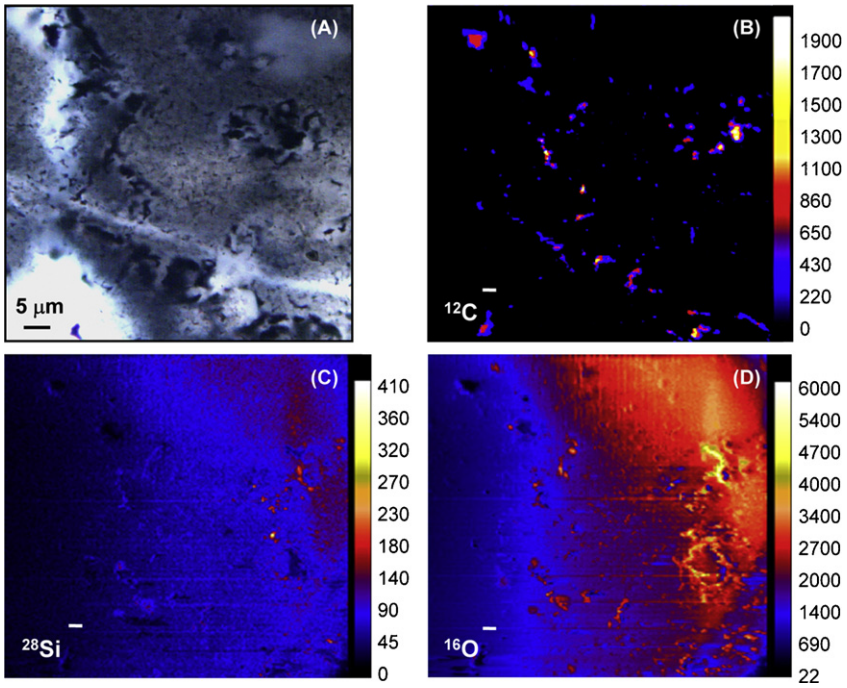

Fig. 4. NanoSIMS images illustrating additional portion of the secondary vein in Member 4 of the Strelley Pool Chert. (A) Optical micrograph of the area imaged in NanoSIMS (B–D); white rectangle in Fig. 1I shows location of this view. (B–D) NanoSIMS element maps; enhancement of carbon image (B) along black particles seen in (A) is not matched by significant enhancement in Si image (C); rather Si image shows apparent lows in the positions of carbonaceous particles. (C) and (D) show that sputtering was uneven in this view with apparently greater sputtering in upper right corners, as evidenced by greater intensity of responses for both Si and O of the chert in that region. While the O image suggests little enhancement of O associated with the carbonaceous particles, some apparent enhancement (restricted to the left sides of some carbonaceous particles) may be an edge effect, due to the uneven sputtering. Color bars and scales indicate intensity of NanoSIMS response. Scales on images are set by the image processing software. Scale bar in (A) applies to (A–D). C, carbon; Si, silicon; O, oxygen.

tration provide strong support for the biogenicity of the Archaean spheroid.

In contrast, the dark material in the secondary vein of the Strelley Pool Chert appears quite distinct. The element maps (Fig. 1J, K) show the dark material to comprise relatively angular, dispersed particles with sharply defined boundaries. There is no evidence of alignment of fragments to form any sort bounding structure. Compared to the Farrel Quartzite spheroid, the particles in the vein are nitrogen-poor (with N/C ratios 1/3–1/4 that of the spheroid), and perhaps most significantly, maps for C and CN (Fig. 1J, K) show an antithetic relationship for these two elements, with the CN response being high only in the narrow, C-poor rims that line the particles (also compare CN/C ratio of Fig. 1L with C image of Fig. 1J). This antithetic relationship may suggest that the N in the rims has a different origin from the C that makes up the bulk of the particles, and in this regard, the particles in the vein are unlike the material comprising both the Archaean and Proterozoic spheroids.

A major difference between the Neoproterozoic and Archaean materials is that the Neoproterozoic Bitter Springs microfossils have C and CN yields an order of magnitude higher than those for the Archaean spheroid or material in the secondary vein (Fig. 1). Since the NanoSIMS analyses for the Archaean and Neoproterozoic materials were obtained at different times, the yields may not be strictly comparable (since element yields depend on NanoSIMS instrument conditions). Nevertheless, a similar difference in yields was observed on a separate suite of samples in SIMS analyses (C. House, personal communication, 2008). Though the cause of the low yields is uncertain, one explanation would be that it is related to a greater degree of diagenetic alteration of the Archaean samples. In contrast, N/C ratios of the Archaean spheroid (0.0125–0.050) are higher than those of the Bitter Springs spheroid (0.0073–0.0133). While this also could be related to age or metamorphic grade of the Archaean spheroid, it might reflect uniquely Archaean biology or perhaps nitrogen cycles (cf., Beaumont and Robert, 1999). Finally, because of the very low yields of both carbon and nitrogen in the Archaean samples, the possibility should be considered that the high N/C ratios could be artifacts due to trace amounts of nitrogen in the vacuum system of the NanoSIMS. This seems unlikely, however, as the hydrothermal vein (with C yield nearly as low as in the spheroid) does not show equivalently high N/C ratios. These possibilities will be evaluated in continuing NanoSIMS studies.

The enhanced Si and O responses in association with the walls of the Bitter Springs spheroids is surprising. Initially, a possibility was considered that kerogen may have remained physically higher in the thin sections than the surrounding chert (due to a greater propensity of chert to take the polish during section preparation) and this, coupled with potentially incomplete sputtering of the gold coating, may have resulted in artifactual enhancement of Si and O at the edges of topographically high kerogen. With continued evaluation, however, this seems unlikely to explain the enhanced Si and O responses. First, the Si and O responses in the chert matrix of some of the microfossils analyzed are not zero (Fig. 2D, E), as would be expected if some of the gold coating remained, covering everything but "high-standing" kerogen. Second, and more important, the enhancement of Si and O, in association with C and CN of the microfossil walls, continues with depth into the thin section (Fig. 2F–H). This is demonstrated by the NanoSIMS responses before and after intense sputtering. Fig. 2F shows the C response obtained in initial NanoSIMS analysis of the Bitter Springs spheroids. Fig. 2G, H shows the C and Si responses of the same sample after intense sputtering, which removed ~1 μm from the surface of the section. It would be expected that, as a result of such deep sputtering, the gold coating would be completely removed and the kerogen could no longer be topographically high. Nevertheless, the intensely sputtered spheroids continue to be characterized by high Si and O (O not shown) responses at the cell walls, suggesting that Si and O enhancement is unlikely to be an artifact of surface topography and incomplete removal of the gold coating.

One explanation is that the enhancement of Si reflects the intimate association between organic matter and silica that results from the process of silica permineralization. This process involves nucleation of silica on organic surfaces, with initial weak bonding between the silica and functional groups in biological materials. Silica permineralization of biological structures is well known from (1) laboratory experiments (Oehler and Schopf, 1971; Oehler, 1976; Toporski et al., 2002), (2) observations of natural silica nucleation on modern microbes (Phoenix et al., 2000; Benning et al., 2002; Renaut et al., 2002), and (3) electron microscopic analyses of ancient microfossils (Moreau and Sharp, 2004). The latter study by Moreau and Sharp shows this intimate relationship in spheroidal microfossils from ~2 Ga Gunflint Formation, where the wall comprises kerogen intimately intermixed with silica. The silica in the walls is very fine-grained (100 nm by 300 nm) compared to the larger crystals (750 nm by 1000 nm) in the chert matrix, and similar size relationships have been observed in many other studies of organic matter and silica (Altermann and Schopf, 1995; Kempe et al., 2005; Oehler and Logan, 1977).

Such intimate intermixing of fine-grained silica and kerogen seems most likely to account for the enhanced Si and O response in the walls of the Bitter Springs microfossils. The mechanism by which this occurs could be due to a "matrix effect" in NanoSIMS where Si and O from the silica associated with kerogen ionize more readily than Si and O from the silica in the matrix chert. Such preferential ionization could result from the comparatively small size of silica grains associated with the kerogen and/or the weak bonding at the kerogen-silica interface. Alternatively, since carbonaceous material is known to sputter faster than chert (Dr. C. House, personal communication, 2008), the enhancement may result from the more rapid sputtering of the organic material during analysis, allowing comparatively more silica mixed with the kerogen of the cell wall to be exposed to the primary ion beam. In either case, the enhanced response of Si and O would be an indicator of an intimate association between silica and kerogen and thus would likely reflect the process of silica permineralization of biological materials.

In contrast, Si associated with carbonaceous material in the secondary vein does not show enhancement over the Si yields in the chert matrix (Figs. 3E, 4C). While the O response in Fig. 3D does show enhancement at the edges of some of the particles, that response occurs only in association with the carbon-poor, nitrogen-high rims that line the particles. The chemical nature of the rims is unknown as is the source of the oxygen within them. The second example of particles in the vein shows no significant enhancement in either Si or O over the responses from the silica matrix (Fig. 4).

A plausible explanation of the difference in Si and O responses of the vein material versus those in both the Bitter Springs and Farrel Quartzite spheroids would be that Si and O enhancement corresponding to kerogenous wall-like structures only results when silica and organic carbon are intimately intermixed, as occurs when silica nucleates as very small crystals on functional groups of biologically derived chemicals. If this is correct, then enhanced Si and O responses in association with ancient carbonaceous material implies that organic matter with remaining functional groups was present in the sediment at the time of silicification. This, in turn, provides an important indicator of syngeneity of the organic matter with silica in the chert matrix. Since Si and O images of the Archaean small spheroid show enhancement comparable to that observed in the Bitter Springs spheroids, this argues that the small spheroids in the Archaean samples were present in the sediment at the time of silicification of the enclosing chert matrix. Accordingly, the organic matter of the small spheroids is unlikely to be an epigenetic contaminant; rather, it is interpreted as being syngenetic with the mineral matrix and thus approximately 3 Ga in age.

5. Conclusions

The similarities in NanoSIMS element distributions of the Archaean small spheroid and Neoproterozoic spheroidal microfossils from the Bitter Springs Formation are suggestive of a biological derivation for the spheroid in the Archaean Farrel Quartzite. In particular, the parallel variations in C and CN concentrations argue for a common origin for carbon and nitrogen that is consistent with an origin from biologically derived materials. The alignment of the partially contiguous, globular C and CN concentrations is additionally reminiscent of enveloping wall-like structures, and as such, strengthens the case for biogenicity of the Archaean spheroid.

The enhancements of Si and O along with C and CN of the Archaean spheroid suggest that the Farrel Quartzite structure is syngenetic with the chert matrix and not a product of any sort of epigenetic contamination. The concomitant differences with the secondary, hydrothermal material in the vein from the Strelley Pool Chert are consistent with the view that the small spheroid in the Farrel Quartzite is likely to be both biogenic and syngenetic.

These conclusions illustrate the applicability of NanoSIMS to assessing biogenicity and syngeneity of structures that might otherwise be difficult to interpret by traditional petrographic methods because of their small size or poor preservation. While small bits of organic matter can be assessed with other techniques (e.g., optical and electron microscopy or Laser Raman imagery), the advantage of NanoSIMS is that both concentration and spatial distributions of several elements (e.g., carbon, nitrogen, sulfur, silicon, and oxygen) can be acquired, and with sub-micron resolution. This combination of high resolution spatial information coupled with concentration data provides a new level of information and accordingly, new insights relative to origins and significance (e.g., see discussion in Oehler et al., 2006 regarding Si associated with spheroidal versus filamentous microfossils from the Bitter Springs Formation).

Conclusions from this study support previous interpretations of Sugitani et al. (2007) that small spheroids in the Farrel Quartzite are probable Early Archaean microfossils. These NanoSIMS results, therefore, add to the growing body of data suggesting that the Archaean biosphere was diverse and well-established by ~3–3.4 Ga (Allwood et al., 2006; Schopf et al., 2007; De Gregorio and Sharp, 2007; Love, 2007; Derenne et al., 2008).

In sum, the comparison of NanoSIMS results from the Farrel Quartzite spheroid and Bitter Springs microfossils illustrates the applicability of this technique to interpreting ancient and poorly preserved materials. New insights have been provided regarding both biogenicity and syngeneity of controversial Archaean structures. These types of analyses should be especially useful as the search for life's origin extends to older and less well preserved samples and even to extraterrestrial materials.

Acknowledgements

We thank the Astromaterials Research and Exploration Science Directorate at NASA-Johnson Space Center (JSC) and Centre National de la Recherche Scientifique (CNRS) for support. Discussions with Dr. Christopher House (Pennsylvania State University) were most helpful in assessing Si and O responses in NanoSIMS. The manuscript was reviewed by Drs. Carlton C. Allen (NASA–JSC), Laurent Remusat (California Institute of Technology and Laboratoire d'Etude de la Matière Extraterrestre, CNRS), Wladyslaw Altermann (Ludwig Maximilians University of Munich) and Christopher House (Pennsylvania State University), all of whom provided insightful comments and excellent suggestions. Dr. Remusat additionally assisted with the image processing software. We also thank Professor J. William Schopf (University of California at Los Angeles) for inviting D.Z.O. to the World Summit on Ancient Microscopic Fossils, as discussions of this work with other participants in that meeting

were most valuable. This work was supported by a PNP grant from the CNRS to F.R., a NASA Fellowship to D.Z.O., and NASA's Exobiology Program.

References

Allwood, A.D., Walter, M.R., Kamber, B.S., Marshall, C.P., Burch, I.W., 2006. Stromatolite reef from the Early Archaean era of Australia. Nature 441, 714–718.

Altermann, W., Schopf, J.W., 1995. Microfossils from the Neoarchean Campbell Group, Griqualand West Sequence of the Transvaal Supergroup, and their paleoenvironmental and evolutionary implications. Precambr. Res. 75, 65–90.

Benning, L.G., Phoenix, V., Yee, N., Tobin, J.J., Konhauser, K.O., Mountain, B.W., 2002. Molecular characterization of cyanobacterial cells during silicification: a synchrotron-based infrared study. Geochem. Earth's Surf. 6, 259–263.

Beaumont, V., Robert, F., 1999. Nitrogen isotope ratios of kerogens in Precambrian cherts: a record of the evolution of atmosphere chemistry? Precambr. Res. 96, 63–82.

De Gregorio, B.T., Sharp, T.G., 2007. *In situ* correlated electron and x-ray microscopy of putative Archean biosignatures: a novel approach for assessing the biogenicity of ancient organic matter. GSA. Abs. Prog. 39 (6), 166–173.

Derenne, S., Robert, F., Skrzypczak-Bonduelle, A., Gourier, D., Binet, L., Rouzaud, J.-N., 2008. Molecular evidence for life in the 3.5 billion year old Warrawoona chert. Earth Planet. Sci. Lett. 272, 476–480.

Fagerbakke, K.M., Heldal, M., Norland, S., 1996. Content of carbon, nitrogen, oxygen, sulfur and phosphorus in native aquatic and cultured bacteria. Aquat. Microb. Ecol. 10 (1), 15–27.

Fukuda, R., Ogawa, H., Nagata, T., Koike, I., 1998. Direct determination of carbon and nitrogen contents of natural bacterial assemblages in marine environments. Appl. Environ. Microbiol. 64 (9), 3352–3358.

House, C.H., Schopf, J.W., McKeegan, K.D., Coath, C.D., Harrison, T.M., Stetter, K.O., 2000. Carbon isotopic composition of individual Precambrian microfossils. Geology 28 (8), 707–710.

Kempe, A., Wirth, R., Altermann, W., Stark, R.W., Schopf, J.W., Heckl, W.M., 2005. Focussed iion beam preparation and *in situ* nanoscopic study of Precambrian acritarchs. Precambr. Res. 140, 36–54.

Love, G.D., 2007. Kerogen-bound aromatic hydrocarbons as potential molecular biosignatures for overmature organic matter in 3.43 Ga Strelley Pool Cherts from Pilbara Craton, Western Australia. GSA. Abs. Prog. 39 (6), 166–175.

Moreau, J.W., Sharp, T.M., 2004. A transmission electron microscopy study of silica and kerogen biosignatures in 1.9 Ga gunflint microfossils. Astrobiology 4 (2), 196–210.

Mojzsis, S.J., Arrhenius, G., McKeegan, K.D., Harrison, T.M., Nutman, A.P., Friend, C.R.L., 1996. Evidence for life on Earth before 3800 million years ago. Nature 384, 55–59.

Oehler, D.Z., Robert, F., Mostefaoui, S., Meibom, A., Selo, M., McKay, D.S., 2006. Chemical mapping of Proterozoic organic matter at sub-micron spatial resolution. Astrobiology 6 (6), 838–850.

Oehler, D.Z., Robert, F., Meibom, A., Mostefaoui, S., Selo, M., Walter, M.R., Sugitani, K., Allwood, A., Mimura, K., Gibson, E.K., 2008a. "Nano" scale biosignatures and the search for extraterrestrial life. 39th Lunar and Planetary Science Conference, Abstract No. 1303.

Oehler, D.Z., Robert, F., Meibom, A., Mostefaoui, S., Selo, M., Walter, M.R., Sugitani, K., Allwood, A., Gibson, E.K., 2008b. NanoSIMS sheds light on the origin and significance of early archean organic microstructures from the Pilbara of Australia. AbSciCon 2008, Abstract No. 8-19-0. Astrobiology 8 (2): 324.

Oehler, D.Z., Robert, F., Chaussidon, M., Gibson, E.K., 2008c. Bona fide biosignatures: Insights from combined NanoSIMS-SIMS. In: Goldschmidt Conference, Vancouver, 2008, p. A698 (Abstract).

Oehler, J.H., 1976. Experimental studies in Precambrian paleontology: Structural and chemical changes in blue-green algae during simulated fossilization in synthetic chert. Geol. Soc. Am. Bull. 87, 117–129.

Oehler, J.H., Logan, R.G., 1977. Microfossils, cherts, and associated mineralization in the Proterozoic McArthur (H.Y.C.) lead-zinc-silver deposit. Econ. Geol. 72 (8), 1393–1409.

Oehler, J.H., Schopf, J.W., 1971. Artificial microfossils: experimental studies of permineralization of blue-green algae in silica. Science 174, 1229–1231.

Phoenix, V.R., Adams, D.G., Konhauser, K.O., 2000. Cyanobacterial viability during hydrothermal biomineralization. Chem. Geol. 169 (3–4), 329–338.

Renaut, R.W., Jones, B., Tiercelin, J.J., Tarits, C., 2002. Sublacustrine precipitation of hydrothermal silica in rift lakes: evidence from Lake Baringo, central Kenya Rift Valley. Sediment. Geol. 148, 235–257.

Robert, F., Oehler, D., Chaussidon, M., Mostefaoui, S., Meibom, A., Gibson, E., 2008. Obtaining valid data from NanoSIMS and SIMS for assessment of early archaean biogenicity. In: XV International Conference on the Origin of Life (ISSOL), 24–29 August, 2008, Florence, Italy.

Schopf, J.W., 1968. Microflora of the bitter springs formation, late Precambrian, central Australia. J. Paleontol. 42 (3), 651–668.

Schopf, J.W., Blacic, J.M., 1971. New microorganisms from the bitter springs formation (late Precambrian) of the north-central Amadeus Basin Australia. J. Paleontol. 45 (6), 925–961.

Schopf, J.W., Kudryavtsev, A.B., Czaja, D., Tripathi, A.B., 2007. Evidence of Archean life: stromatolites and microfossils. Precambr. Res. 158, 141–155.

Sugitani, K., Grey, K., Allwood, A., Nagaoka, T., Mimura, K., Minami, M., Marshall, C.P., Van Kranendonk, Walter, M.R., 2007. Diverse microstructures from Archaean chert from the Mount Goldsworthy-Mount Grant area, Pilbara Craton, Western Australia: microfossils, dubiofossils, or pseudofossils? Precambr. Res. 158 (3–4), 228–262.

Toporski, J.K., Steele, A., Westall, F., Thomas-Keprta, K.L., McKay, D.S., 2002. The simulated silicification of bacteria—new clues to the modes and timing of bacterial preservation and implications for the search for extraterrestrial microfossils. Astrobiology 2 (1), 1–26.